Paschen's Law in Air and Noble Gases

L. F. Berzak, S. E. Dorfman, and S. P. Smith

April 25, 2006

Abstract

Paschen curves for air, helium, neon, and xenon are obtained by measuring the breakdown voltage of gas within a Pyrex vacuum vessel with two planar, stainless steal electrodes. Data is taken at various pressures and electrode separations and fit to a Paschen curve. The constants A' and B are extracted both from the fit and from examining the minimum of the experimental curve. The trends in the shapes of the curves are examined and explained based on the electrochemical properties of the various gases. Despite showing similar trends, our measurements differed from the reported values by as many as five standard deviations. Future experiments using more precise, automated voltage adjustment are proposed to correct for these deviations.

1 Introduction

In 1889 Friedrich Paschen published what is now known as Paschen's Law [1]: the breakdown voltage, V_B between two electrodes is a function of pd, the product of the pressure inside the chamber and the distance between the electrodes. He derived the following relation:

$$V_B = \frac{Bpd}{\ln(Apd/\ln(1/\gamma))}. \tag{1}$$

A, B, and γ are constants to be discussed below.

To understand the physical process behind Paschen's Law, consider a vacuum chamber in which breakdown has not yet occurred. There may be several free electrons in the chamber due to external ionizing sources such as cosmic rays. If a voltage is applied across the tube, a free electron will begin to accelerate towards the anode. If the gas is sufficiently dense, the electron may collide with a neutral atom, causing ionization. The resulting positive ion accelerates towards the cathode; when it collides with the electrode, there is a finite probability (γ) that a secondary electron will be emitted. This secondary electron may in turn ionize more neutrals; the positive ions that result will stream towards the cathode. If each electron, on average, creates enough ions to release at least one additional secondary electron from the cathode, the process becomes self-sustaining, and breakdown occurs.

A graph of equation (1) as a function of pressure is shown as the blue curve in figure 1 for $A = 1$, $B = 2$, $\gamma = 0.1$, and $d = 3$. To the left of the minimum, the breakdown voltage decreases with increasing pd. Here, the gas is not very dense or the plates are very close; thus, even if a large number of secondary electrons are emitted, there is a low probability that any will collide with neutral atoms during the journey from the cathode to the anode. As pd increases, collisions are more likely, and therefore the breakdown voltage is lower; thus, the Paschen curve has a negative slope in this region.

When pd increases beyond the curve's minimum, collisions may be too frequent rather than too rare. In this regime, an electron on its way to the anode may collide so frequently that a larger input voltage is required for it to build up enough energy to ionize a neutral atom. The electron-neutral collision frequency and thus the voltage required increases with pd, explaining the positive slope of the Paschen curve at large pd.

Solving for the minimum of equation (1) with respect to pd:

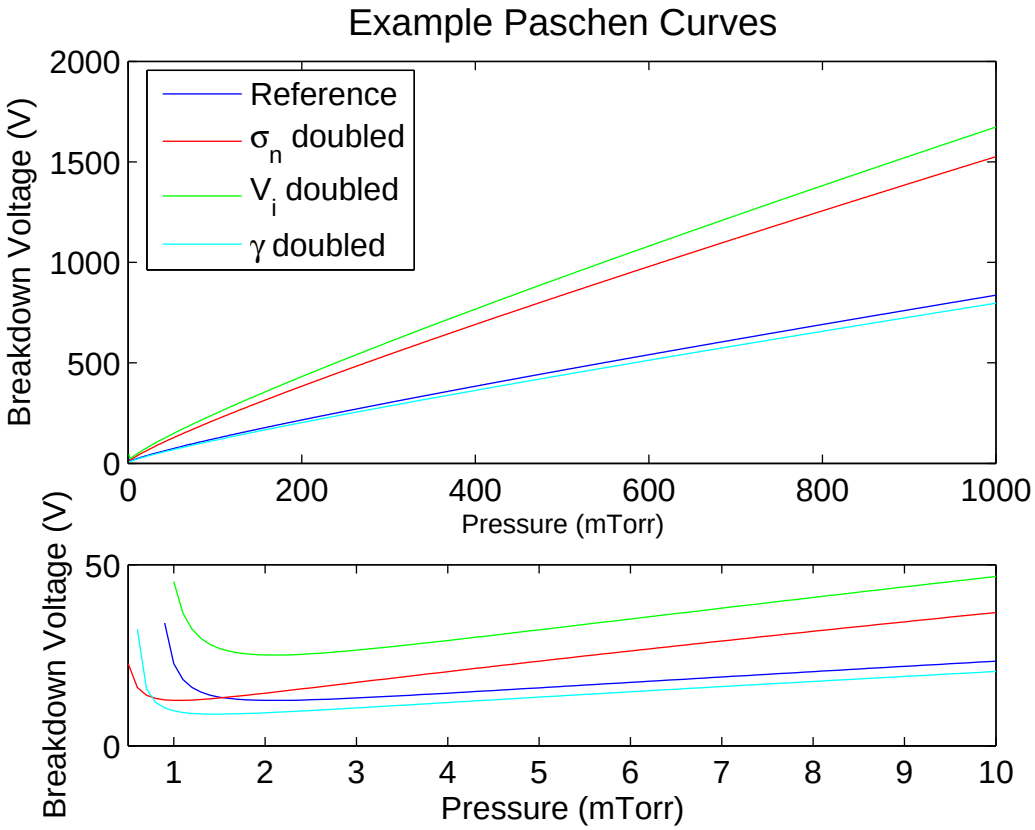

Figure 1: Plots of equation (1) as a function of pressure for various parameters as explained in the text.

$$(V_B)_{min} = \frac{\exp(1) B \ln(\frac{1}{\gamma})}{A} \tag{2a}$$

$$(pd)_{min} = \frac{\exp(1) \ln(\frac{1}{\gamma})}{A} \tag{2b}$$

Three key parameters in the breakdown process are the electron-neutral collisional cross section σ_n, the ionization potential V_i, and the secondary electron emission coefficient γ. In equation (1), the first two parameters are contained in the constants $A = \frac{\sigma_n}{kT_n}$ and $B = AV_i$ where T_n is the temperature of the neutral atoms, and k is Boltzmann's constant.

The red and green curves in figure 1 illustrate the effect of doubling σ_n and V_i, respectively. Comparing the red and blue curves, a larger σ_n translates to more frequent collisions which lowers the breakdown voltage for low pd, but raises it for high pd. Thus, $(pd)_{min}$ shifts left. By contrast, a change in V_i has the same effect in both regions; large V_i means that fewer electrons will have enough energy to ionize a neutral during a collision. Thus, it makes sense that the entire curve including $(V_B)_{min}$ shifts up as seen from a comparison of the blue and green traces.

The result of doubling γ is shown by the cyan curve in figure 1. The change has very little effect in the high pd region where the limiting factor is the energy of a secondary electron rather than the number of such electrons. In the low pd region, the frequency of electron-neutral collisions is too low prior to breakdown; a larger γ means more secondary electrons, thus more collisions, and therefore a lower breakdown voltage. Synthesizing the trends in the two regions, we conclude that $(pd)_{min}$ shifts left and $(V_B)_{min}$ shifts down for increasing γ.

Various atoms and molecules will have different σ_n, V_i, and γ depending on their electronic properties. For example, moving down the noble gas column in the periodic table, V_i decreases while the atomic radius and hence σ_n increases. The γ dependence is less clear, as different sources [2, 3] make opposing claims. By observing the trends in the low pd region, high pd region, $(V_B)_{min}$, and $(pd)_{min}$, we can determine which of the three parameters has the most influence as well as the correct trend in γ. For example, $(V_B)_{min}$ should decrease moving down the column based on the trend in V_i; however, $(V_B)_{min}$ could increase if γ is decreasing fast enough.

To explore these concepts, we measured the Paschen curves of three noble gases and air in a cylindrical vacuum chamber by varying the pressure and/or distance and measuring the resultant breakdown voltage.

2 Experiment

2.1 Experimental Apparatus, Methods, and Results

The apparatus for measuring the breakdown voltage at varying pressure and electrode spacing is shown in figure 2. The circular planar electrodes used were stainless steel with a diameter of ~ 10 cm. The electrode distance was varied by means of a rotary feedthrough. The pressure was finely varied

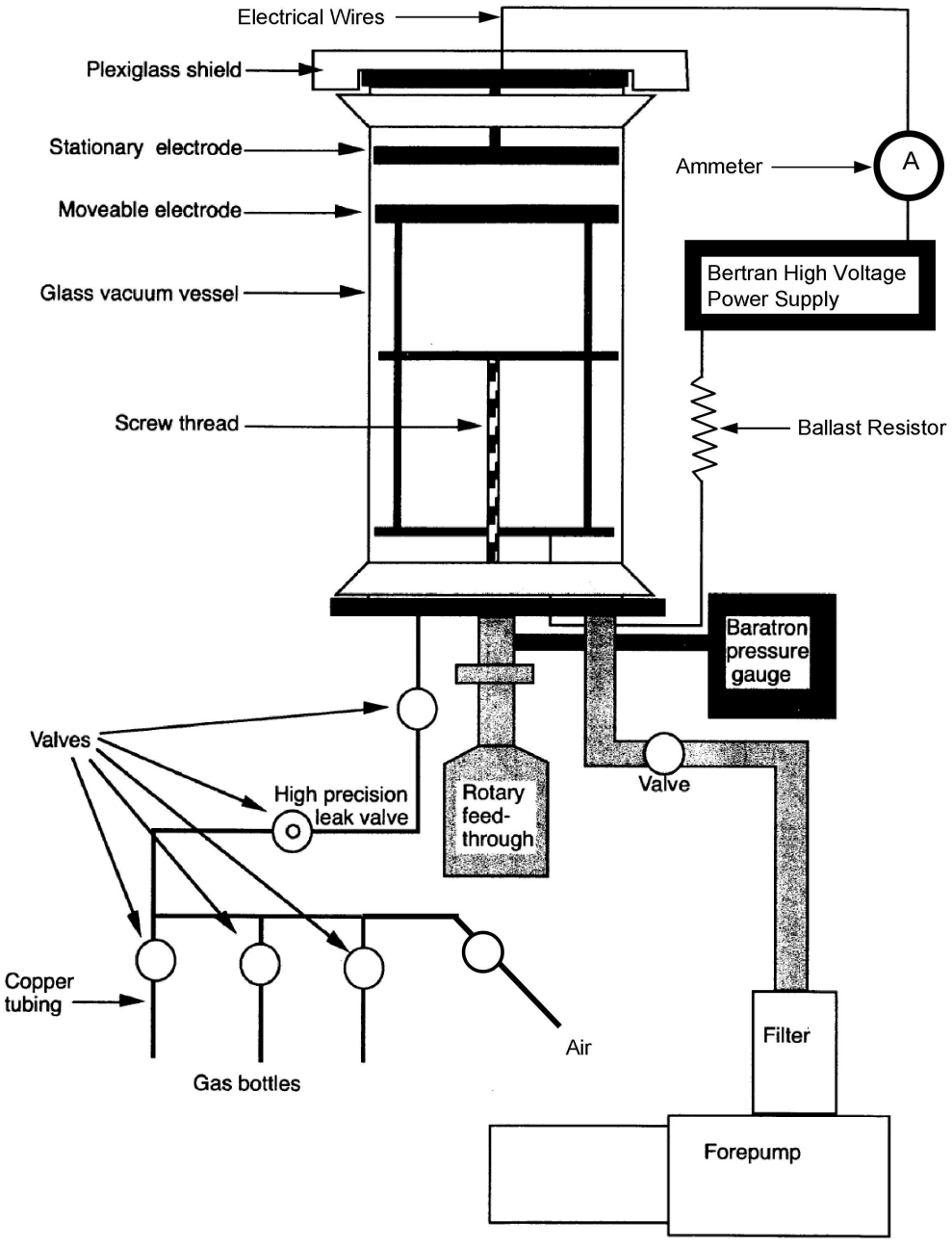

Figure 2: Experimental Apparatus. Figure adapted from lab manual[2].

Gas	Spacing (cm)		Pressures (torr)	
	Min	Max	Min	Max
Air	0.50	5.00	0.283	2.924
Helium	3.00	3.00	0.507	10.825
Neon	3.00	3.00	0.186	3.429
Xenon	1.50	5.00	0.124	7.556

Table 1: The ranges of electrode spacing, d, and pressures, p, of the given gases for which the breakdown voltage, V_B, was determined.

using a high precision leak valve. Table 1 shows the ranges of electrode spacing and pressures for each of the gases used: air, helium, neon, and xenon. When switching between gases, the Pyrex vacuum chamber and lines were flushed with the new gas at least four times before taking breakdown voltage data. The purity of the new gas in the chamber was qualitatively determined by comparing the spectrum of the subsequent plasma (observed with a very simple diffraction grating) with the known spectrum of the new gas and the spectrum of the gas previously in the chamber.

To find the breakdown voltage for a given pressure, p, and electrode spacing, d, the voltage applied to the electrodes was manually increased until a current was observed on the ammeter, indicating that the circuit had been closed by the formation of a plasma. Even though there was a voltage drop across the ballast resistor, the drop was proportional to the current, which was negligible at the time of plasma formation. Thus, the applied voltage for which the plasma formed was recorded as the breakdown voltage [4]. The procedure was repeated multiple times for each distance and pressure, and the average breakdown voltage calculated. The results for all gases, pressures, and distances are shown in figure 3. A description of the plasmas observed is found in Appendix A.

Values of $A' \equiv A/\ln(1/\gamma)$ and B for each gas were determined by fitting a curve of the form (1) to the breakdown voltage data. The fits along with the data are shown in figure 4. A' and B were also calculated from equations (2) as

$$A' = \frac{\exp(1)}{(pd)_{min}} \tag{3a}$$

$$B = \frac{(V_B)_{min}}{(pd)_{min}} \tag{3b}$$

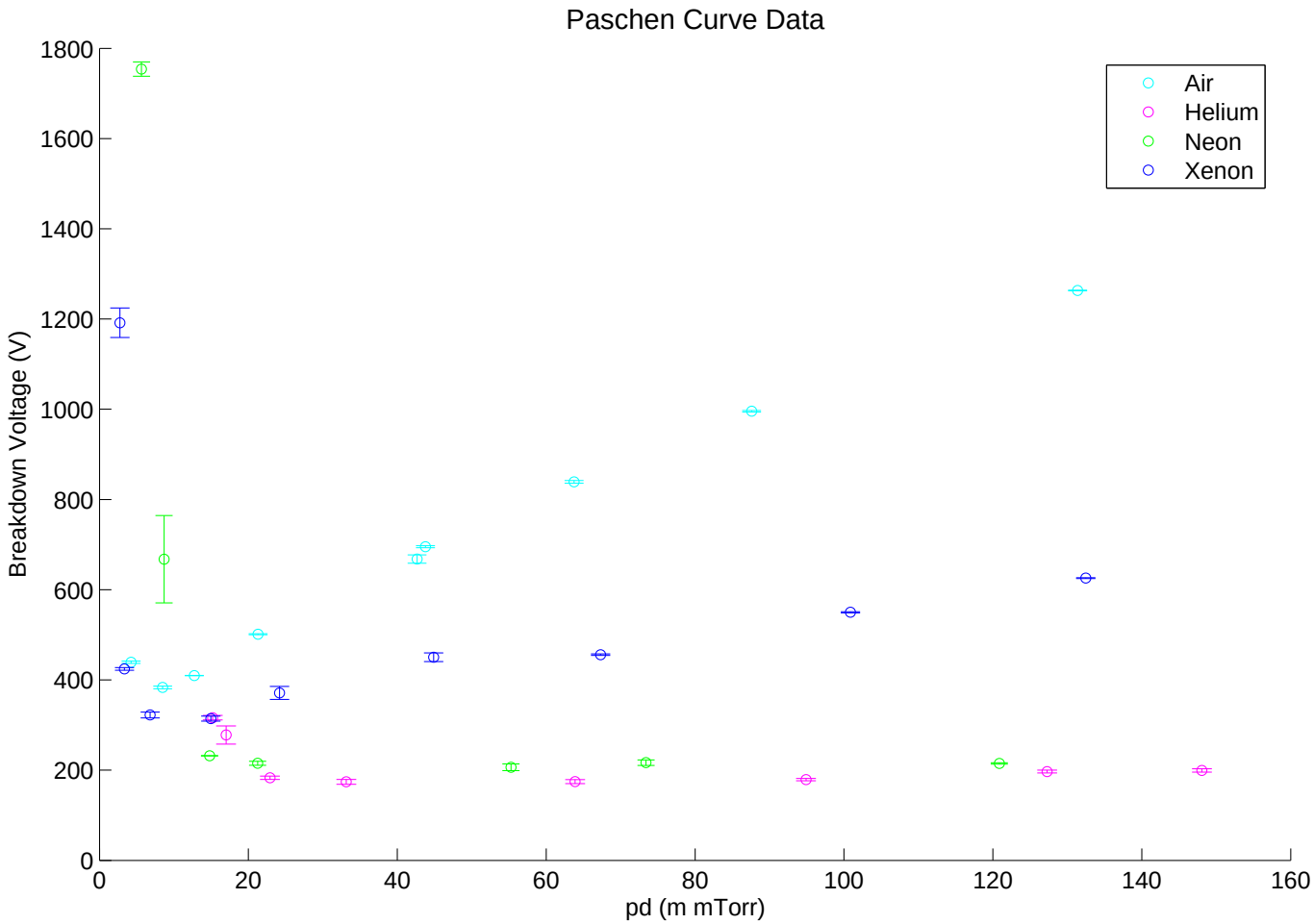

Figure 3: Breakdown voltage as a function of the product, pd.

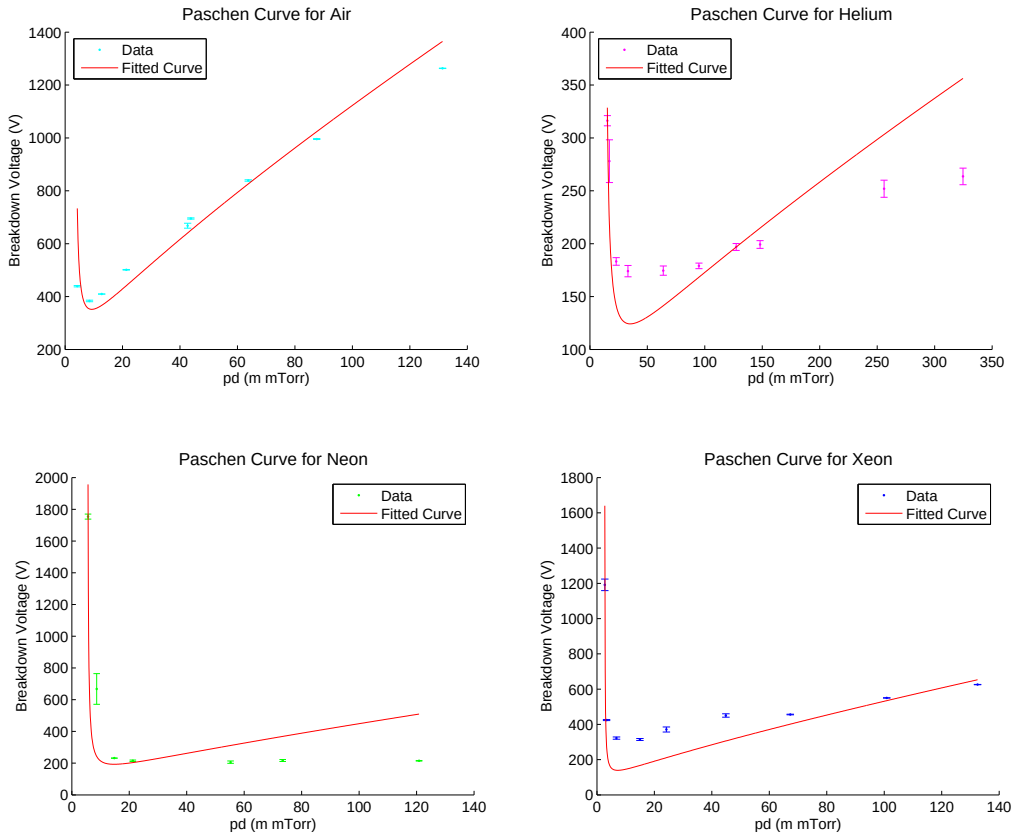

Figure 4: Experimental Paschen curves with the theoretical fit given by (1) with the values of A' and B given in table 2.

The calculated and reported [2] values of A' and B are presented in table 2. One particular trend for the noble gases is that for increasing atomic radius, A' and B from the fitted curves both increase.

2.2 Error Analysis

One source of uncertainty in this experiment comes from the inablility to obtain a pure gas in the chamber, or at least the inability to quantify the composition. While steps were taken to flush the system, as previously

Gas	A' $\left(\frac{1}{\text{m mTorr}}\right)$		
	Reported[2]	Fit	Minimum
Air	0.38	0.29 ± 0.02	0.32
Helium	0.067	0.077 ± 0.002	0.08
Neon	—	0.184 ± 0.006	0.49
Xenon	—	0.376 ± 0.008	0.27

Gas	B $\left(\frac{\text{V}}{\text{m mTorr}}\right)$		
	Reported[2]	Fit	Minimum
Air	36	38 ± 2	45
Helium	3.4	3.5 ± 0.2	5.3
Neon	—	13 ± 2	38
Xenon	—	19.3 ± 0.8	29

Table 2: Values of $A' \equiv A/\ln(1/\gamma)$ and B calculated by fitting (Fit) the breakdown voltage to an ideal Paschen curve (see equation (1)) or by calculating the minimum in the Paschen curve (see equations (3)).

mentioned, it is likely that there remained impurities embedded in the apparatus. These impurities could be desorbed either through natural outgassing or through a sputtering process wherein the pure gas ion strikes the electrode and dislodges the impurity.

The error bars of figure 3 can be attributed to human error, pressure variability, stray sources of ionization radiation, and gas composition; a description of each follows. Inevitably, there was a delay (small, but finite and variable) between when the plasma was formed and when the person stopped turning the dial on the voltage source. The pressure variability is most noticeable at low pd where $|\partial V_B/\partial pd|$ is the greatest. When the applied voltage is not too far below the breakdown voltage, a stray source of radiation could ionize enough neutrals to produce breakdown. Finally, even with slight gas composition changes, σ_n and V_i will vary, leading to a differently shaped Paschen curve.

3 Discussion

Comparison of the calculated values of A' and B with the reported values indicates that the values are of the correct order and exhibit the same trends. The differences between the curve-fit values and the minimum calculation values are indicative of the variability of analytical methods, showing the importance of cross-checking calculations. In addition, examining the Paschen curves themselves permits analysis of the expected qualitative trends. The noble gas trend is as follows: increasing $(V_B)_{min}$ and decreasing $(pd)_{min}$ as one moves down the periodic table from helium. The trend in $(V_B)_{min}$ seems counter-intuitive given that the ionization potentials of the gases decrease from helium to neon to xenon. However, the ionization potential is only the energy required to remove the outermost valence electron, while the breakdown voltage is truly a complicated mixing of multiple effects, as described in the introduction. These effects include γ, the secondary electron emission coefficient for ions striking the cathode. Although the lab manual indicates that γ increases as one moves down the periodic table [2], another source indicates that γ actually decreases as the gas's ionization potential decreases [3]. It may be possible, then, that the observed trend in $(V_B)_{min}$ for the noble gases is due to the effect of decreasing γ. The trend in $(pd)_{min}$ may also be rationalized on physical grounds. This value is dependent on the parameters as indicated in equation (2b). Because A is dependent on collision cross-section (σ_n), as the size of the gas atoms/molecules increases and thus the size of the respective σ_n increases, the value of $(pd)_{min}$ should decrease, as is indeed observed.

Air is even more complex to consider than the noble gases since air's molecular and atomic content is uncertain. The Paschen curve for air had the highest $(V_B)_{min}$ and the leftmost $(pd)_{min}$, but air has the lowest ionization potential and a mid-range γ [2]. To explain these effects, first, it must be remembered that the voltage applied across the plasma does not only go into electron removal; rather, vibrational and rotational states of molecules may be excited as well [6]. Thus, the excitation of these additional degrees of freedom must lead to air's high $(V_B)_{min}$. That air has the leftmost $(pd)_{min}$ value is an interesting observation. This may indicate that air has the largest σ_n of all the gases studied here, and indeed this makes physical sense as air is a mixture of many gases including numerous larger molecules.

Although great care was exercised during the data taking and qualitative trends are apparent, deviations between reported values of A' and B and

calculated values are as many as five standard deviations. This is disappointing, but indicative of the variability of the experiment. Thus, it would be interesting in future experiments to design an automated device which could slowly and evenly adjust the voltage applied across the cathode and anode, stopping immediately once a set current was drawn. This would allow the data to be taken more regularly and permit greater confidence in the measured breakdown voltages. In addition, since Paschen's law is dependent on gas type, it would be valuable to have a spectrometer, in addition to the diffraction grating, which would allow experimenters to determine the true composition of the working medium and what percentages of each gas are present. The percentages of impurity gas could then be lessened through baking out the chamber and vacuum system whenever the working medium is changed, and by utilizing a turbo pump when the experiment is not being run in order to keep the chamber clean. Lastly, it would be interesting to repeat the experiment for different types of cathodes, such as the hollow cathode. This would give one the opportunity to further examine the architecture of a glow discharge as well as to better understand the physical processes associated with breakdown.

This experiment provided the opportunity to investigate one of the most fundamental plasma processes, namely plasma formation. Using several different gases, we were able to measure the differences in breakdown voltages. Although the resulting data was not ideal, the value of the experiment was not lessened. The data still permitted the clarification of the breakdown process and allowed the experimenters to deeply consider sources of error and uncertainty, as well as ways to alleviate these in the future.

References

[1] V.A. Lisovskiy, S.D. Yakovin, and V.D. Yegorenkov, "Low-pressure Gas Breakdown in Uniform DC Electric Field," J. Phys. D, **33** (2000), 2722.

[2] S Cohen, "D.C. Breakdown of Gases: Paschen Curves."

[3] R Hackam, "Total Secondary Ionization Coefficients and Breakdown Potentials of Monatomic Gases between Mild Steel Coaxial Cylinders", J. Phys. B, **2** 2 (1969) 201.

[4] G Auday, Ph Guillot, J Galy, and H Brunet, "Experimental Study of the Effective Secondary Emission Coefficient for Rare Gases and Copper Electrodes," J. Appl. Phys., **83** 11 (1998), 5917.

[5] L. F. Berzak, S. E. Dorfman, and S. P. Smith, "Chaos and Periodicity in a Neon Glow Discharge", Unpublished (2006).

[6] A. von Engel, *Ionized Gases*, Oxford University Press (London, 1955), Ch. 7.

A Description of Plasmas

During the experiment, we observed two distinct types of discharge - an abnormal glow and a normal glow. The abnormal glow occurred at higher pressures and covered the cathode, while the normal glow occurred at lower pressures and appeared as moving 'spots' of plasma on the cathode. It was observed that these spots were often not stationary, and the movement for some discharges was even periodic in nature. We were able to measure the period of the motion and found that not only did the period vary between discharges, but the direction of motion changed as well. This was, qualitatively, an intriguing phenomenon and would certainly be of interest and scientific value to investigate further.

For the abnormal discharges, it often occurred that the positive column filled nearly all of the space between the electrodes. We did not observe striations, such as those observed previously [5]. However, we did note that the color of the discharge was not uniform. While the different gases produced differently colored discharges (air was pink and purple; helium was light blue at low pressures and white-gray at high pressures; neon was an orange shade; and xenon was lavendar-gray), the discharge for a single gas tended to be brighter and lighter towards the cathode. Also, as we continued investigating various combinations of pressure and electrode spacing, we attempted to decrease the value of pd by both decreasing the pressure and decreasing the spacing. If the spacing was decreased below ~ 1.5 cm, rather than observing a discharge between the two electrodes, it appeared that the discharge was above and on the sides of the cathode, perhaps exhibiting the arcing phenomenon. Consequently, we were required to utilize larger spacings than this minimum.

B I-V Traces

In addition to measuring data to make the requisite Paschen curves, we also measured I-V characteristics of the plasma (once breakdown was achieved). The I-V characteristics were linear for most of the discharges, with a slope of ~ 100. This slope corresponds to the value of the ballast resistor in series with the plasma, and the linear nature of the plots indicates that the voltage across the plasma remains nearly constant as the current

increases. In the normal discharge, this makes intuitive sense as the current density flowing to the cathode remains approximately constant as the total current varies, thus the 'spots' on the cathode will increase in area with the increase in total current leading to only a slow change in voltage. However, a similar linear behavior was also observed for the abnormal discharges. It is important to note, though, that this abnormal discharge linear behavior tended to have a smaller slope than the normal discharge's linear behavior. The linear behavior of the normal glow traces leads one to surmise that the resistivity (ρ) (and hence conductivity ($\sigma = \frac{1}{\rho}$) of the plasma remains approximately constant for the density and temperature regimes examined here. Since

$$V_{plasma} = IR_{plasma} = jA\frac{\rho L}{A} = j\rho L$$

and V_{plasma}, j, and L are all roughly constant, ρ must also be roughly constant. Interestingly, the conductivity σ goes as:

$$\sigma \propto \frac{ne^2}{m\nu_{ei}} \text{ where } \nu_{ei} \propto \frac{ne^4 v_t}{T^2} \text{ and } v_t \propto \sqrt{\frac{T}{m}} \Longrightarrow \sigma \propto \frac{T^{\frac{3}{2}}}{e^4 m^{\frac{1}{2}}}$$

Thus, a roughly constant σ indicates that the temperature of a given normal discharge was nearly constant.

C Effective Ionization Potential

Gas	A $\left(\frac{1}{\text{m mTorr}}\right)$	B $\left(\frac{\text{V}}{\text{m mTorr}}\right)$	V_i (V)	$V_{ieff} = \frac{B}{A}$ (V)
H_2	0.54	14	15.4	26
He	0.28	3.4	24.6	12
N_2	1.2	34	15.8	28
Air	1.5	36	13	24
Ar	1.2	18	15.8	15

Table 3: Table 1 from [2] with values of the effective ionization potential calculated.

Table 3 is an adaptation of Table 1 from reference [2]. From the given values of A and B, V_{ieff} was calculated from the relation $B = AV_i$. This

effective ionization potential takes into account deviations from a simple model in which electrons lose all their energy after a collision with a neutral and in which all collisions where the electron has sufficient energy result in ionization. In reality, some collisions may be elastic or excite the atom or molecule in a non-ionizing fashion [6]. For example, diatomic molecules in table 3, with additional molecular degrees of freedom to excite, have a V_{ieff} that is larger than V_i by almost a factor of two.

Using the effective ionization potentials for Air and Helium, it is possible to calculate A and γ from our curve fitting parameters A' and B by making use of $B = AV_i$. For Neon and Xenon, this is not possible since we lack values of V_{ieff}. The A values calculated in this manner are within one standard deviation of the reported values from table 3. Meanwhile, the γ values for Helium and Air are within two and eight standard deviations respectively of the values given in [2].

Gas	A $\left(\frac{1}{\text{m mTorr}}\right)$	γ
Air	1.6 ± 0.2	0.005 ± 0.002
He	0.29 ± 0.02	0.023 ± 0.007

Table 4: A and γ for Air and Helium calculated based on the effective ionization potential.